ACS APPLIED MATERIALS & INTERFACES

Research Article

www.acsami.org

Long-Chain 3,4-Ethylenedioxythiophene/Thiophene Oligomers and Semiconducting Thin Films Prepared by Their Electropolymerization

K. M. Nalin de Silva,[†] Euiyong Hwang, Wilson K. Serem, Frank R. Fronczek, Jayne C. Garno, and Evgueni E. Nesterov*

Department of Chemistry, Louisiana State University, Baton Rouge, Louisiana 70803, United States

Supporting Information

ABSTRACT: A series of soluble H-terminated conjugated oligomers incorporating 3,4-ethylenedioxythiophene (EDOT) combined with a small number of thiophene units and ranging in length from four to eight EDOT/thiophene groups was prepared with the ultimate goal to investigate if facile formation of a reactive trication radical species would enable electrochemical polymerization of such long-chain oligomers. Spectroscopic and electrochemical studies of the oligomers revealed some general dependencies of their electronic properties on the total number and position of EDOT groups. It was the number of consecutive EDOT units rather than total number of these units which was found to have the most profound effect on electronic energy gap and conjugation length. This influence originates from the especially strong planarization induced in the conjugated backbone by the incorporation of EDOT units. In contrast, incorporation of thiophene units was found to result in loss of the conformational stabilization. This phenomenon was analyzed using the natural bond orbital computational approach, which revealed the predominantly hyperconjugative nature of the EDOT-induced conformational stabilization. Whereas shorter oligomers, in agreement with the general consensus, were found to be inert toward electrochemical polymerization due to low reactivity of electrochemically generated cation radical and dication species, the longest oligomer showed an unprecedentedly efficient electropolymerization to yield a stable thin film of an electroactive polymer. The efficient electropolymerization of the long-chain oligomer was found to be in agreement with the formation of a reactive trication radical species. The electronic and spectral properties of the resulting semiconducting polymer film were studied by various electrochemical and spectroelectrochemical methods, as well as conductive probe AFM technique, and revealed a number of unusual features (such as electrical rectifying switching behavior) consistent with the possibility of increased molecular order in this material.

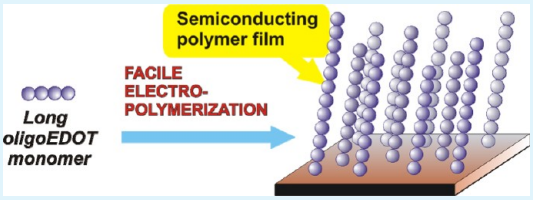

KEYWORDS: *semiconducting polymers, thin films, oligomers, polythiophenes, EDOT, molecular organization*

INTRODUCTION

Organic π-electron conjugated thiophene-based oligomers attract much attention due to their potential applications in thin-film organic electronic and optoelectronic devices.[1−15] Although numerous efforts have been directed toward modification of electronic (i.e., optical and electrochemical) properties of such oligomers for use in devices, only limited attempts have been made to employ presynthesized oligomers as monomers in preparation of conjugated polymers.[16−19] The possibility of using longer oligomers instead of more conventional small molecule monomers would allow access to thiophene copolymers that incorporate functional units in a well-defined precisely controlled manner, rather than in a randomly distributed fashion, with the purpose of modification and fine-tuning of electronic properties of thin-film materials derived from such copolymers.[20−22] In addition, using precisely defined oligomers allows increasing versatility and efficiency of macromolecular design.

The majority of previous efforts to use oligomers in conjugated copolymer preparations utilized chemical polymerization methods (such as transition metal catalyzed coupling routes); and much fewer studies were devoted to electrochemical polymerization. Electropolymerization is a simple and common approach for in situ preparation of both electrode-attached and free-standing polythiophene thin films.[23−25] The main advantage of electropolymerization is that it allows direct conversion of monomers into semiconducting polymer thin films ready for use in electronic devices, without the need first to prepare soluble polymers as required in solution-based thin film fabrication processes. Therefore, it makes unnecessary "decorating" the polymer with bulky solubilizing side groups, which often increase disorder and result in lowering conjugation length in thin-film organic materials, as well as have detrimental effect on their photo- and thermal stability.[26,27] Using long-chain conjugated oligomers instead of small molecule monomers for electropolymerization would have an additional advantage that it could produce thin-film materials consisting of more monodisperse polymer chains, with fewer coupling or conformational defects of the conjugated polymer backbone, thus yielding materials with

Received: July 16, 2012
Accepted: September 12, 2012
Published: September 12, 2012

   dx.doi.org/10.1021/am301349g | ACS Appl. Mater. Interfaces 2012, 4, 5430−5441

better electronic characteristics. The simple basis for this conjecture is that making polymers from long-chain monomers requires fewer coupling steps. For example, using octithiophene as a monomer would require only 10 coupling steps to achieve a polymer with 80 thiophene units, whereas it would require 80 steps if thiophene were used as the monomer. In fact, studies of electropolymerization with various length oligothiophenes have been attempted as early as nearly two decades ago.[28−30] Those studies, however, were complicated by generally low electropolymerization rates with longer thiophene oligomers (beginning with terthiophene) mostly due to the insufficient reactivity of intermediate oligothiophene cation radicals stabilized by extended conjugation, and resulted in low quality of electropolymerized thin films. Indeed, α-terthiophene, α-quaterthiophene, and α-quinquethiophene were all found to be very poorly electropolymerizable, yielding products mainly resulting from dimerization of the initially formed cation radicals.[31−34] On the other hand, a longer monomer, dialkyl-substituted sexithiophene, was found to undergo very efficient electrochemical coupling to produce very high quality polythiophene films (although it was not clear if the coupling actually went beyond simple dimerization).[35] Also, a series of oligothiophenes ranging from 2 to 16 thiophene units was reported to efficiently electropolymerize in the solid state.[36] Replacing thiophene with its 3,4-ethylenedioxythiophene (EDOT) analogue was found to increase oligomers' electropolymerizability. Thus, terEDOT[37] and ter(3,4-phenylenedioxythiophene)[38] readily undergo electrochemical polymerization to form conducting polymer thin films. Despite some differences in interpretation of literature results on this subject, there seems to be a general consensus that long conjugated oligomers are poorly (if at all) electropolymerizable because of the increased stabilization of their extended cation radicals, which prevents further coupling toward the formation of polymers.

On the basis of analysis of the general electropolymerization mechanism and literature data, we hypothesized that whereas not sufficiently long oligomers are indeed not electropolymerizable because of the reasons described above, longer conjugated thiophene oligomers may be readily electropolymerizable. In such a case, the polymerization would occur through the intermediacy of a more reactive trication radical species. It is well-established that in the case of extended conjugated oligomers, trication radical species can be formed upon electrochemical oxidation, albeit only at high positive potentials.[39−41] The higher reactivity of a trication radical (as compared to a cation radical species formed from the same oligomer) does facilitate oxidative coupling of oligomers and their subsequent polymerization; this was, for example, observed in the electrochemical coupling of terfluorene.[42] Although formation of trication radical in relatively short conjugated oligomers is possible only at prohibitively high potentials beyond the practically useful electrochemical range, the more extended conjugation in sufficiently long-chain oligomers can decrease this potential to somewhat lower values.[43] This simple qualitative analysis leads to the hypothesis that gradual increasing of the oligomer's length beginning from a small molecule will first make it unreactive toward electrochemical polymerization because of the progressively increasing stabilization of the cation radical species, but further lengthening will make it polymerizable because of the easier formed reactive trication radical.

To test this hypothesis, we decided to prepare a series of uniformly built oligomers based on 3,4-ethylenedioxythiophene (EDOT) building block and study in detail their properties and, in particular, electrochemical reactivity. The EDOT-incorporating oligomers were selected over purely thiophene-based analogues because of the absence (or steric inaccessibility) of β-hydrogens in EDOT oligomers that would preclude undesired $\alpha-\beta$ coupling during polymerization, since such a coupling could complicate the correct interpretation of electropolymerization results.[44] Also, the presence of EDOT units (especially at terminal positions) in oligomers was expected to additionally facilitate electropolymerization.[45−47] Although a number of soluble EDOT-incorporating oligomers have been described to date, most of them possessed aryl, alkyl, or bulky silyl end-capping groups at the terminal α positions to improve their solubility and increase stability, and therefore were not electropolymerizable.[48−51] In order to be electropolymerizable, a compound should have no substituents at both terminal α-positions (H-terminated). To the best of our knowledge, longer EDOT-based H-terminated oligomers have not been described yet. Therefore, for the present study we prepared and characterized a series of H-terminated oligomers **1**−**5** ranging in length from 4 to 8 thienyl units in their conjugated backbone (Figure 1).

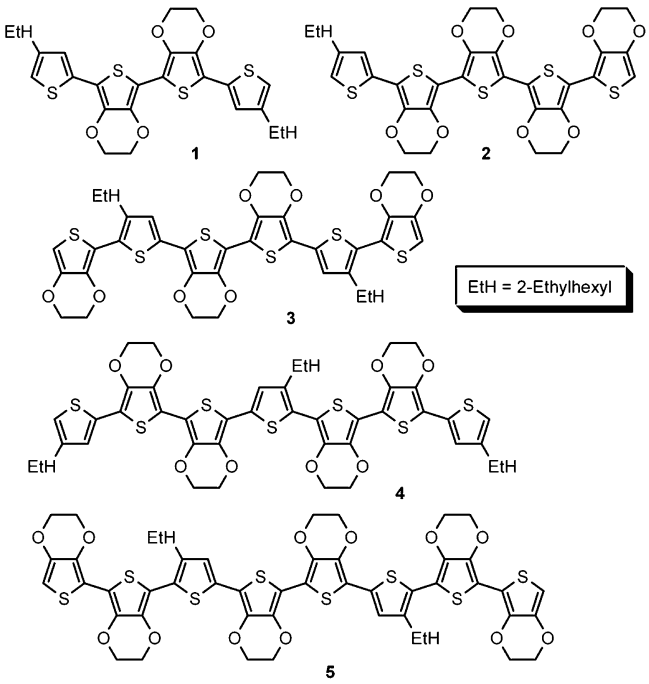

Figure 1. Molecular structures of oligomers **1**−**5**.

EXPERIMENTAL SECTION

Materials and Methods. All reactions were performed under an atmosphere of dry nitrogen. Melting points were determined in open capillaries and are uncorrected. Column chromatography was performed on silica gel (Sorbent Technologies, 60 Å, 40−63 μm) slurry packed into glass columns. Tetrahydrofuran (THF), dichloromethane, ether, and toluene were dried by passing through activated alumina, and *N*,*N*-dimethylformamide (DMF) − by passing through activated molecular sieves, using a PS-400 solvent purification system from Innovative Technology, Inc. The water content of the solvents was periodically controlled by Karl Fischer titration (using a DL32 coulometric titrator from Mettler Toledo). All other solvents were additionally purified and dried by standard techniques. Tetrabutylammonium hexafluorophosphate was obtained from Aldrich and used

dx.doi.org/10.1021/am301349g | ACS Appl. Mater. Interfaces 2012, 4, 5430−5441

after recrystallization from ethanol, other reagents and solvents were obtained from Aldrich and Alfa Aesar and used as received. Indium tin oxide (ITO) coated glass slides with 8−12 Ohm/sq. surface resistivity were purchased from Delta Technologies, Ltd. Au-coated glass slides (100 nm Au on top of 5 nm Cr layer) were purchased from EMF, Inc. Interdigitated microelectrodes (Au electrodes on glass support) were purchased from ABTECH Scientific, Inc. UV−visible spectra were recorded on Varian Cary 50 UV−vis spectrophotometer. Fluorescence studies were carried out with a PTI QuantaMaster4/2006SE spectrofluorimeter. Fluorescence quantum yields were determined relative to methanol solutions of Acridine Yellow (Φ = 0.57[52]) as standard. All electrochemical and spectroelectrochemical experiments were performed using an Autolab PGSTAT 302 bipotentiostat from Eco Chemie. ^{1}H NMR spectra were recorded at 250 MHz, and are reported in ppm downfield from tetramethylsilane. High resolution mass spectra were obtained at the LSU Department of Chemistry Mass Spectrometry Facility using an ESI method, and a peak matching protocol to determine the mass and error range of the molecular ion. Ab initio and DFT computations were performed on Intel Xeon dual-processor computer with Linux OS using Gaussian 03[53] computational package.

Synthesis. Synthetic procedures including complete analytical characterizations are provided in the Supporting Information section.

Electrochemical Measurements. Electrochemical measurements were performed using an Autolab PGSTAT 302 potentiostat with a bipotentiostat module. Unless otherwise noted, all experiments were carried out using a three-electrode system with polymer-modified ITO/glass or Au/glass working electrode (electrode area ∼1.3 cm^2) or interdigitated microelectrode, Ag/AgNO$_3$ nonaqueous reference electrode, and a Pt gauze counter electrode. The reference electrode was checked against ferrocene standard every time before and after the experiments were performed, and the measured potentials were corrected based on the Fc/Fc$^+$ redox potential value. All experiments were carried out in 0.1 M Bu_4NPF_6 solution in CH_2Cl_2 as supporting electrolyte.

Preparation of Electrode Substrates for Electropolymerization. Rectangular ITO-covered glass slides (approximately 1.1 × 2.5 cm) were ultrasonicated in CH_2Cl_2 for 20 min, followed by rinsing with acetone and deionized water. The precleaned slides were subjected to an RCA-type cleaning procedure by keeping in a water −30% H_2O_2 − 30% aqueous NH_3 (5:1:1) mixture at 70 °C for 1 h. The substrates were then rinsed with copious amount of deionized water and dried in N_2 flow at room temperature for 2 h. Au/glass slides were rinsed with MeOH, and successively ultrasonicated in MeOH, acetone, isopropanol (10 min in each solvent), rinsed with deionized water, MeOH, and dried in N_2 flow at room temperature for 2 h.

Preparation and Electrochemical Characterization of Polymers. Electrodeposition of polymers **poly(5)** and PEDOT was accomplished through 5 scans in CV mode using an Au/glass or ITO/glass substrate as a working electrode in 1 mM solution of monomers **5** or bisEDOT, respectively, in 0.1 M Bu_4NPF_6 in CH_2Cl_2, at the scanning rate of 0.1 V s^{-1}. After polymerization was complete, the sample was rinsed with copious amount of CH_2Cl_2 and dried in N_2 flow. The substrate was placed in a monomer-free electrolyte for CV characterization that included 10 successive scans at the scanning rate of 0.1 V s^{-1}. At the end of the last scan, the sample was left at the standby potential of −1.0 V to ensure leaving the polymer in an electrochemically undoped state. The sample was washed with copious amount of CH_2Cl_2 and dried in N_2 flow.

Spectroelectrochemistry. Spectroelectrochemical experiments were conducted using a rectangular quartz cuvette (path length 1 cm) with a polymer-modified ITO/glass working electrode placed inside the cuvette, Pt gauze counter electrode attached around the walls inside the cuvette with a rectangular hole against the sample, and Ag/Ag$^+$ nonaqueous working electrode which was checked against Fc/Fc$^+$ standard immediately before and after measurements. The supporting electrolyte was 0.1 M Bu_4NPF_6 in CH_2Cl_2. Absorption spectra were recorded in 0.1 V potential increments.

Atomic Force Microscopy. Tapping mode and conductive probe images were acquired with an Agilent 5500 AFM/SPM system equipped with Picoscan v5.3.3 software. Rectangular cantilevers from Nanosensors (Lady's Island, SC) were used for tapping mode characterizations, at a driving frequency of 167 ± 3 kHz. Conductive probe AFM (CP-AFM) was used to map the sample conductance while operating in contact mode. The nosecone of the scanner contained a preamp module with 1 nA V^{-1} sensitivity for CP-AFM. Conductive tips with an average force constant of 6 N m^{-1} were used for simultaneous current and contact-mode imaging (MikroMasch CSC11/Ti−Pt, San Jose, CA). The tip coating consisted of a 10 nm layer of Pt on a sublayer of 20 nm Ti, which was coated on both the tip and reflective side of the cantilever. The resulting radius of the tip with the coating was ∼40.0 nm. Topographic and current images were acquired simultaneously with a DC bias voltage range of ±10 V applied to the samples, using a scan rate of 3.0 nm s^{-1} for 512 lines/frame. The set point was chosen at a minimum value to prevent damage to the film and the cantilever. Estimates of surface coverage were made with UTHSCA Image Tool.[54] The percentage of colored pixels provided a relative estimate of surface coverage. The AFM current images were converted to grayscale bitmaps and a threshold value was selected visually for estimates of the percentages of black and white pixels.

X-ray Crystallography. Diffraction data were collected at T = 90 K on a Nonius KappaCCD diffractometer equipped with Mo $K\alpha$ radiation (λ = 0.71073 Å) and an Oxford Cryostream cooler. Crystal data for **1**: Orange plates, $C_{36}H_{46}O_4S_4$, M_r = 670.97, monoclinic space group $P2_1/c$, a = 22.433(3), b = 4.9502(5), c = 16.387(2) Å, β = 111.351(4)°, V = 1694.8(4) Å^3, Z = 2, ρ_{calcd} = 1.315 g cm^{-3}, μ = 0.319 mm^{-1}, 41590 measured data, R = 0.056 ($F^2 > 2\sigma$), R_w = 0.145 for 6073 unique data (4216 observed) having θ < 32.5°, and 194 refined parameters. *Comments:* The molecule lies on an inversion center, thus the central S−C−C-S torsion angle is exactly *anti*. The terminal thiophene units are nearer to *syn*, with torsion angle 15.1(2)°. One of the 2-ethylhexyl groups is disordered into two conformations, only one of which is illustrated in Figure 2.

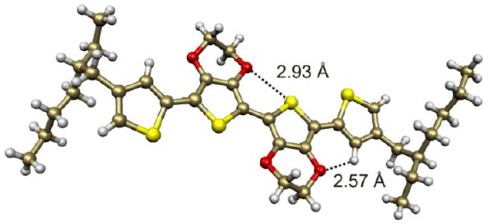

Figure 2. Molecular structure and conformation of tetramer **1** derived from single-crystal X-ray data.

RESULTS AND DISCUSSION

Synthesis and Structure of Oligomers. Purely oligoEDOT compounds are practically insoluble, indeed according to literature data,[37] even the trimer (terEDOT) has very low solubility in organic solvents. In the course of the present study, we have initially prepared hexaEDOT which was found to be completely insoluble in any solvent, and its identity could only be established by mass-spectral experiments. Therefore, it was necessary to introduce a minimal number of solubilizing groups into the oligomers. Although it could be more appropriate to add solubilizing alkyl substituents to the ethylenedioxy fragment of an EDOT unit, this would require substantially more complex synthetic preparations. Also, oligomers combining both EDOT and thienyl units have been shown to possess interesting electronic properties,[48] therefore it would be conceivable to study possibility of preparing semiconducting polymers from such oligomers. Thus, each EDOT oligomer **1**−

5 was chosen to incorporate one or two β-(2-ethylhexyl)thienyl units. This provided sufficient solubility even to the longest oligomers, while still mostly preserving the oligoEDOT nature of them. The convergent synthetic approach chosen to prepare the oligomers (vide infra) resulted in some oligomers (compounds **1**, **2**, and **4**) being terminated with β-(2-ethylhexyl)thienyl rather than EDOT units. Although this potentially could affect their electrochemical polymerization ability relative to the EDOT-terminated oligomers **3** and **5**, our computational analysis indicated that it might have only a minor influence. In particular, we carried out gas-phase geometry optimizations of the neutral oligomers **1** and **5**, as well as their cation radicals, at the B3LYP/6-31G* level (this level of theory was proven satisfactory for accurate computational treatment of π-electron conjugated oligomers[55]). The highest occupied molecular orbital (HOMO) in the neutral molecules and the spin density in the cation radicals showed similar distribution in both oligomers, without any significant differences between terminal β-(2-ethylhexyl)thienyl units in **1** and EDOT terminal units in **5** (see Figure S2 in the Supporting Information). Thus, at least at this level of theoretical treatment, we could not observe any major effect of the two alternative terminal groups on the oligomers' electrochemical reactivity.

The oligomers were prepared by traditional convergent synthesis where some of the shorter oligomers were used as precursors for the longer ones (see the Supporting Information for details). Regiochemistry of 2-ethylhexyl substituents in tetramer **1**, which was critical for correct assigning the structure for the oligomers **3** and **5**, was additionally proven by single crystal X-ray analysis (Figure 2). In this structure, the completely coplanar central EDOT units were in *anti* conformation with respect to each other, and the dihedral angle between the terminal thienyl and EDOT units was 15°. It is generally accepted that incorporating EDOT units into a conjugated oligothiophene system gives rise to intramolecular noncovalent interactions resulting in self-rigidification and planarization of the conjugated system.[56] Interestingly, the terminal thienyl units were found to exist in the less thermodynamically favorable *syn* conformation with EDOT units. Theoretical calculations at B3LYP/6-31G* level revealed that this conformation is slightly (~1.3 kcal mol^{-1}) less stable than the corresponding all-*anti* conformation. It has been proposed,[48,57] that *anti* orientation of adjacent EDOT units is additionally stabilized by the attractive through-space interactions between S and O atoms of the two EDOT groups, as compared to similar oligothiophenes. Indeed, in the X-ray-derived structure we found a relatively short (2.93 Å) S···O distance between two central EDOT units, which was substantially shorter than the sum of the van der Waals radii of the S and O atoms (3.35 Å), and might be an indication of the existence of such interactions. By analogy, similar interactions between the S atom of a terminal thienyl unit and the O atom of the adjacent EDOT unit could provide stabilization for an all-*anti* conformation in **1**. On the other hand, a relatively short (2.57 Å) distance between hydrogen in the β position of a terminal thienyl ring and the oxygen of an adjacent central EDOT unit (Figure 2) could indicate existence of a weak C–H···O hydrogen bond, providing a means for alternative stabilization of the experimentally observed *syn* conformer.

Since remarkably stabilized planarized conformation is a general feature of EDOT-containing oligomers, we decided to investigate the origin of the conformational stabilization by performing full geometry optimization (at B3LYP/6-31G* level) and analysis utilizing the Natural Bond Orbital (NBO) method,[58] which proved to be a useful theoretical tool in deciphering intramolecular donor–acceptor and hyperconjugative interactions. For the *anti* oriented central EDOT groups, NBO analysis did not find any substantial interactions between filled orbitals at the S atom of one EDOT group and antibonding orbitals involving O atoms of another EDOT group (which would reflect stabilizing S···O interactions). Instead, a pair of hyperconjugative interactions between almost antiperiplanar orbitals $\sigma_{S1-C2} \rightarrow \sigma^*_{S1'-C2'}$ and $\sigma_{S1'-C2'} \rightarrow \sigma^*_{S1-C2}$ with an interaction energy (determined as a second order perturbation) ranging between 4.0 – 4.2 kcal mol^{-1} per interaction was found to strongly stabilize this *anti* conformation (Figure 3A). Similarly strong hyperconjugative

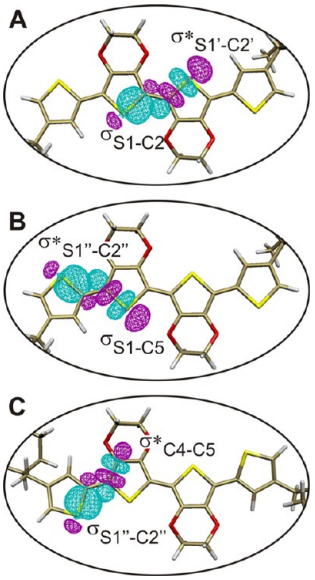

Figure 3. NBO analysis of stabilizing hyperconjugative interactions (A, B) in the all-*anti* conformer of **1**, and (C) in the experimentally found conformation with *syn* orientation between terminal thienyl and EDOT groups. The computations were performed at B3LYP/6-31G* level.

stabilization was found between the *anti*-oriented terminal thiophene and the central EDOT units in the all-*anti* conformer (average interaction energy for $\sigma_{S1-C5} \rightarrow \sigma^*_{S1''-C2''}$ and $\sigma_{S1''-C2''} \rightarrow \sigma^*_{S1-C5}$ around 4.2 kcal mol^{-1}, Figure 3B). In addition to the hyperconjugative interactions, strong electrostatic attraction between oppositely charged S and O atoms of the adjacent EDOT groups (NBO charges +0.45 for S and −0.53 for O) likely provides extra stabilization for the planar *anti* conformation of the two central EDOT units. Therefore, this additional electrostatic stabilization is probably the major reason behind the enhanced backbone planarity and rigidity when EDOT units are introduced into thiophene oligomers and polymers.

For the experimentally found conformation with *syn* orientation of the terminal thiophene and central EDOT units, the hyperconjugative interactions between significantly less antiperiplanar orbitals ($\sigma_{C2-C3} \rightarrow \sigma^*_{S1''-C2''}$ and $\sigma_{S1''-C2''} \rightarrow \sigma^*_{S1-C5}$, Figure 3C) provide noticeably lower stabilization, as compared to the compound in an all-*anti* conformation, with a stabilization energy ranging from 2.7 to 3.2 kcal mol^{-1} per

dx.doi.org/10.1021/am301349g | ACS Appl. Mater. Interfaces 2012, 4, 5430–5441

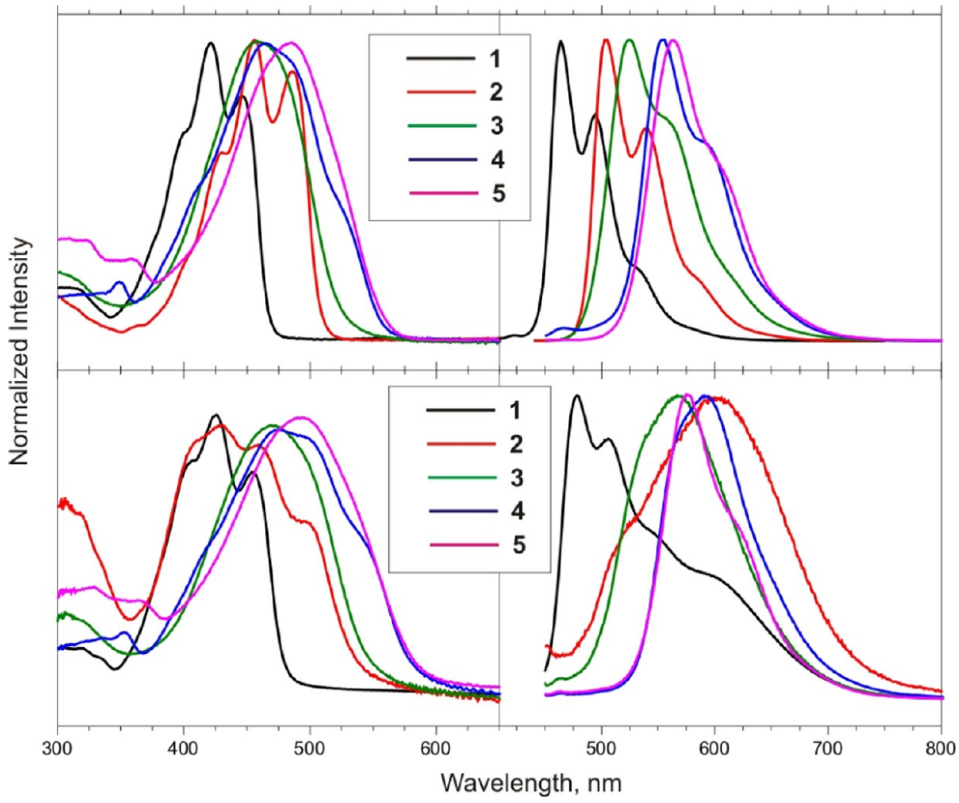

Figure 4. Normalized absorption (left) and fluorescence (right) spectra of oligomers **1**−**5** in CH_2Cl_2 solution (top row) and in thin film (bottom row).

Table 1. Spectroscopic and Electronic Properties of Oligomers 1−5

	solution[a]		thin film						
compd	λ_{abs}, nm (ε, × 10^4, $M^{-1}cm^{-1}$)	λ_{em}, nm (Φ, %)	λ_{abs} (nm)	λ_{em},(nm)	$E_{pa}1/E_{pa}2$, (V)[b]	E_{HOMO} (eV)[c]	E_{LUMO} (eV)[d]	E_g^{opt} (eV)[e]	E_g^{DFT} (eV)[f]
1	422 (4.81)	464 (11)	427	477	0.38/0.85	−5.09	−2.47	2.62	2.90
2	456 (5.85)	505 (17)	430	600	0.01/0.62	−4.72	−2.32	2.40	2.63
3	461 (2.50)	527 (14)	469	569	0.22/0.56	−4.93	−2.66	2.27	2.52
4	467 (6.58)	556 (22)	476	590	0.05/0.50	−4.76	−2.58	2.18	2.38
5	485 (7.83)	567 (15)	490	575	0.09/0.50	−4.80	−2.64	2.16	2.32

[a]Measured in 1 μM solutions in CH_2Cl_2. [b]First and second anodic oxidation peak potentials, measured in a standard three-electrode cell for 1 mM solutions in 0.1 M Bu_4NPF_6 in CH_2Cl_2 using a Pt button electrode and Ag/Ag^+ reference electrode. [c]Calculated using formula $E_{HOMO} = -(E_{pa}1 + 4.71)$ (eV). [d]Calculated based on the corresponding values of E_{HOMO} and E_g^{opt}. [e]Determined as long wavelength onset of absorption spectra. [f]Calculated at B3LYP/6-31G* level of theory based on gas-phase geometry optimized with the same method.

interaction. The difference between the interaction energies roughly accounts for the computed 1.3 kcal mol^{-1} higher stability of the all-*anti* conformer. Although the energy difference between the two conformers is really small and can be easily overcome by the gain from better intermolecular organization in single-crystalline phase, it does confirm the prevalence of the hyperconjugatively stabilized all-*anti* conformation for EDOT-containing oligomers and polymers.[48,49,56,59]

Optical and Electrochemical Properties of Oligomers. Absorption and fluorescence spectra of oligomers **1** − **5** in CH_2Cl_2 solution and in spin-cast thin films are shown in Figure 4, and the data are summarized in Table 1. As expected, absorption and emission maxima shift bathochromically with increasing length of oligomers. The magnitude of the shift depends both on the total length and on the number of the adjacent EDOT units; thus, the biggest relative shift between a pair of oligomers differing by one thienyl/EDOT unit (34 nm) was observed on going from **1** (two adjacent EDOT groups) to **2** (four adjacent EDOT units). At the same time, increasing the oligomer's length without increasing the number of adjacent EDOT units showed a smaller effect on the position of the absorption maximum, even with increasing the total number of (nonadjacent) EDOT groups. This observation illustrates the major role of adjacent EDOT units in enforcing a planarized and more rigid molecular conformation with more extended π-electron conjugation, whereas on the other hand, incorporation of a thienyl group between EDOT units results in enhancing rotational/vibrational freedom, which detrimentally affects conjugation length. Although shorter compounds **1** and **2** showed typical for rigid systems well-resolved vibronic structure in absorption and emission spectra, longer oligomers displayed featureless bands due to inhomogeneous broadening caused by increased conformational freedom.[60] Furthermore, all oligomers except pentamer **2** showed no substantial intermolecular electronic interactions in solid films as evidenced by

the similarity between their solution and spin-cast thin-film spectra (Figure 4). The absence of aggregation features in thin-film spectra can be seen as an indication of a significant rotational freedom of the thienyl units, leading to existence of nonplanar, conformationally twisted species in solid films. On the other hand, four consecutively connected EDOT units in pentamer **2** induce a very rigid and planar molecular geometry, facilitating formation of low-emissive aggregated species in the solid state, with typical broadening of the absorption spectrum, and an almost 100 nm bathochromically shifted featureless emission band. As the absorption maximum continuously bathochromically shifted from tetramer **1** to octamer **5**, so did the energy bandgap E_g^{opt} showed continuous increase (Table 1). The number of consecutively connected EDOT units, rather than total number of EDOT units, had the most profound effect on the energy gap. Hence, the relative difference was biggest between tetramer **1** and pentamer **2**, whereas it became more modest on transition to higher oligomers, even despite an increase in the total number of EDOT groups. To gain insight on the dependence of the energy gap on structural features of the oligomers, computational geometry optimizations were carried out at B3LYP/6-31G* level of theory on gas phase molecules in the all-*anti* conformation of thienyl and EDOT units. The calculations produced stable planar geometries, even for the longest oligomer **5**. The energy gap values E_g^{DFT} calculated assuming planarized geometry were in good agreement with experimentally determined optical energy gaps E_g^{opt} (Table 1) and showed a quantitative trend to decrease with an increasing number of EDOT/thienyl units. This supports the idea of a relatively planar geometry of oligomers **1**−**5** in dilute solutions.

The electrochemical properties of oligomers **1**−**5** were studied by cyclic voltammetry (CV) in dichloromethane solutions. All oligomers showed two successive reversible one-electron reduction processes corresponding to formation of a radical cation and dication (Table 1 and Figure 5). The relatively low values of the oxidation potentials (especially for the longest oligomer **5**) indicated strong stabilization of the oxidized species. Paralleling the tendency in the optical energy gap change, the electrochemical HOMO energy determined from the first anodic oxidation peak $E_{pa}1$ showed strong dependence on the number of consecutively connected EDOT units. Thus, the HOMO energy significantly increased upon transition from **1** to **2**, but dropped noticeably on transition from **2** to **3**, and showed some smaller increase for **4** and **5**.

Electrochemical Polymerization. In good agreement with our initial hypothesis, the shorter oligomers **1**−**4** were found to be nonelectropolymerizable upon repeated CV scanning over a broad potential range (Figure 5A), whereas the longest oligomer **5** turned out to electropolymerize very efficiently. The polymerization of **5** could be carried out potentiodynamically both on flat Au and indium tin oxide (ITO) working electrodes, to yield mechanically and electrochemically stable dark-blue (when polymerization was stopped at −1.4 V to get electrochemically undoped material) films of polymer **poly(5)**. Successive potential cycling of an octamer **5** solution led to development of a new sharp redox peak at $E_{1/2}$ −0.47 V (vs Ag/Ag^+ reference electrode), representing a reversible redox process of the newly deposited **poly(5)** (Figure 5B, C). Comparison of absorption spectra of an undoped film of **poly(5)** with those of monomer **5** and of the reference polyEDOT (PEDOT) polymer prepared by electropolymerization of bisEDOT[61] indicated an extended conjugated nature of

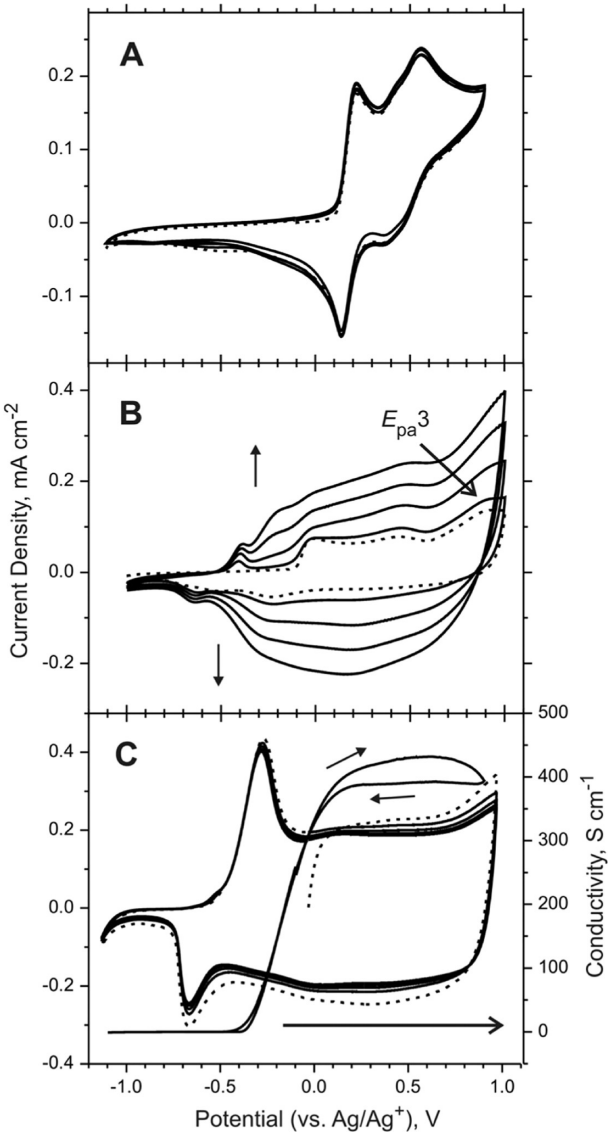

Figure 5. Cyclic voltammograms (5 successive scans) of oligomers (A) **3** and (B) **5**, and (C) polymer **poly(5)** on flat Au electrode. Experimental conditions: concentration 1.24 mM (**3**) and 1.0 mM (**5**) in 0.1 M Bu_4NPF_6 in CH_2Cl_2, scanning rate 0.1 V s^{-1}. Dash traces in each plot correspond to the first scan. In addition, plot C shows in situ conductivity data of **poly(5)** as thin film prepared by electropolymerization on interdigitated Au microelectrodes; experimental conditions: 0.1 M Bu_4NPF_6 in CH_2Cl_2, scan rate 5 mV s^{-1}.

poly(5) (thus proving **poly(5)** is a real polymer) (Figure 6A). The deposited **poly(5)** films were found to be electrochemically stable and did not show significant changes upon successive CV scanning (Figure 5C). This served as a proof that **poly(5)** was a long and oxidatively stable polymer (rather than a mixture of short-chain electrochemically unstable oligomers, which would continue to polymerize in the solid film) and suggested a high extent of electronic delocalization. The sharp well-defined reversible peak for anodic oxidation likely reflected a relatively narrow distribution of conjugation lengths in this polymer owing to fewer coupling steps required to obtain a high molecular weight polymer from the long-chain monomer **5**. The peak current was found to show linear dependence on the scan rate, to indicate that the electroactive **poly(5)** films were strongly adhered to the electrode surface.

dx.doi.org/10.1021/am301349g | ACS Appl. Mater. Interfaces 2012, 4, 5430−5441

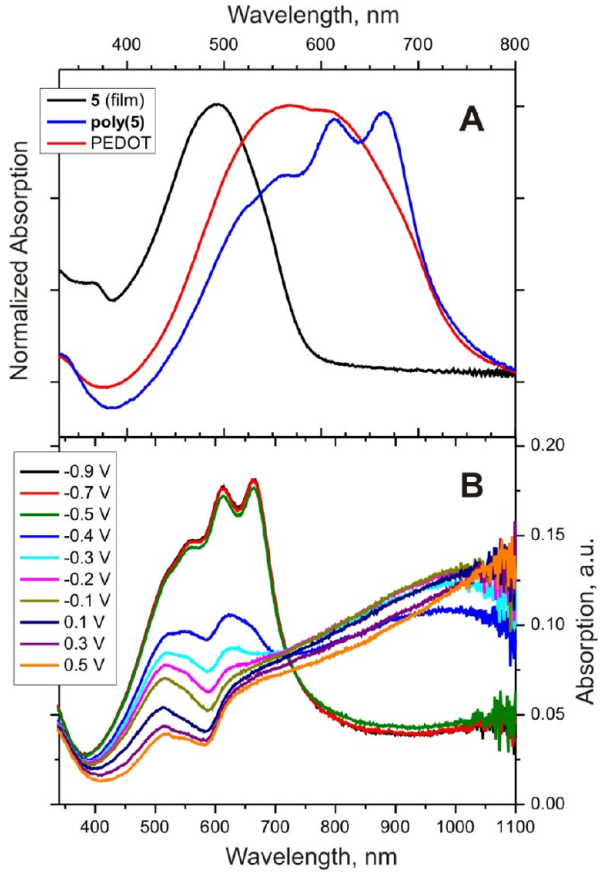

Figure 6. (A) Absorption spectra of thin film polymer **poly(5)** and reference thin films of PEDOT and monomer **5**. (B) Spectroelectrochemistry of **poly(5)** prepared by potentiodynamic electropolymerization on ITO-coated glass slides from a 1 mM solution of monomer **5** in 0.1 M Bu_4NPF_6 in CH_2Cl_2; the potentials were measured vs Ag/Ag^+ quasi-reference electrode.

The facile electropolymerization of oligomer **5** was remarkable considering strong stabilization of its cation radical as evidenced by the low value of $E_{pa}1$. Thus, it is very likely that formation of the more reactive trication radical was responsible for the facility of electropolymerization of **5**. Indeed, the experimentally observed third anodic oxidation peak $E_{pa}3$ at 0.93 V in the cyclic voltammogram of **5** could be assigned to the trication radical formation (Figure 5B); this peak was not present in the CV data for shorter oligomers **1**–**4**, and the low value of its potential was in agreement with our initial hypothesis and with previous literature data.[43] To prove the key role of possible formation of trication radical upon reaching $E_{pa}3$ in effecting polymerization, we carried out a series of experiments where the positive end potential of CV scanning range was increased from 0.6 V (well above the potential required to form cation radical and dication species of **5** but well below the 0.93 V potential required to form the trication radical) to 1.3 V in 0.1 V steps. There was no polymer formation observed in the experiments where the end potential was set below 0.9 V, however, deposition of the semiconducting polymer film began in the experiments when the positive end scanning potential reached the value of 0.9 V of the $E_{pa}3$. The best quality polymer film was obtained when CV potential was cycled in the range from −1.0 to 1.0 V; a further increase in the positive end potential resulted in lower quality polymer, probably because of the electrochemical degradation of **poly(5)** at higher potentials. This observation supports the requirement to form reactive trication radical as the species responsible for the electropolymerization of the long-chain oligomer **5**.

Spectroscopic and Electrochemical Characterization of Poly(5). In the electrochemically undoped, insulating state, **poly(5)** showed a broad π–π^* transition in the range of 400–800 nm (Figure 6A), with the optical bandgap determined from the onset of absorption estimated at 1.6 eV, which agrees well with the bandgap values found both experimentally and computationally for PEDOT polymers.[62,63] While the magnitude of the optical bandgap primarily reflects a significant extent of intramolecular π-electron conjugation, the presence of well-defined vibronic structure (as opposed to broad featureless absorption band typically found in PEDOT polymers[64]) serves as a strong indication of an enhanced molecular order along the conjugated backbone in the polymer's thin layer.[65−67] Furthermore, the long wavelength onset of the absorption band for **poly(5)** was found to be noticeably steeper than that of PEDOT polymer prepared by electropolymerization of bisEDOT in similar conditions (Figure 6A). These details are consistent with a more narrow distribution of conjugation lengths in the thin film of **poly(5)**, which facilitates predominantly band-edge electronic transitions and is characteristic of more ordered and better aligned conjugated polymer chains.[68,69]

In spectroelectrochemical studies, absorption spectra of the electrodeposited film of **poly(5)** were first obtained in the fully reduced (undoped) state of the polymer, and then were recorded as the potential was gradually stepping up toward oxidized (polaron and bipolaron) states (Figure 6B). The polymer demonstrated complete reversibility of spectral changes upon multiple switching between oxidized and reduced forms. As the potential was stepped up, the π–π^* transition band of the neutral state was observed to gradually decrease, and was replaced first with a broad band centered around 900 nm corresponding to polaronic transition, which, in turn, was superseded at higher potentials by an intense bipolaronic band positioned in the near-IR region. An interesting feature was that **poly(5)** exhibited almost a threshold, in a narrow potential interval, electrochromic switching between colored reduced and almost UV/vis transparent oxidized forms. This spectroelectrochemical behavior of **poly(5)** was consistent with its narrow anodic redox peak found in CV experiments (Figure 5C). It could be attributed to the more ordered polymer backbone organization in the thin film of **poly(5)**, with lesser defects, more planarized conformation of the polymer chains and more narrow distribution of conjugation lengths. Indeed, generation of cation radical (polaron) and bipolaron species with their quinoidal structure requires planarization of the conjugated polymer backbone; therefore the initially more planar molecular geometry of **poly(5)** would greatly facilitate the charge carrier formation.

In situ conductivity measurements were carried out with thin films of **poly(5)** electrodeposited on interdigitated microelectrodes (Figure 5C).[70,71] The value of maximum conductivity found in these experiments (around 400 S cm^{-1}), although it should be treated cautiously because of serious intrinsic limitations of the in situ measurements, was in agreement with the values reported for electrodeposited PEDOT polymers.[64] Interestingly, polymer **poly(5)** showed practically no hysteresis for forward and reverse switching. The absence of hysteresis was in good correlation with the narrow insulating–conducting state switching interval found for this

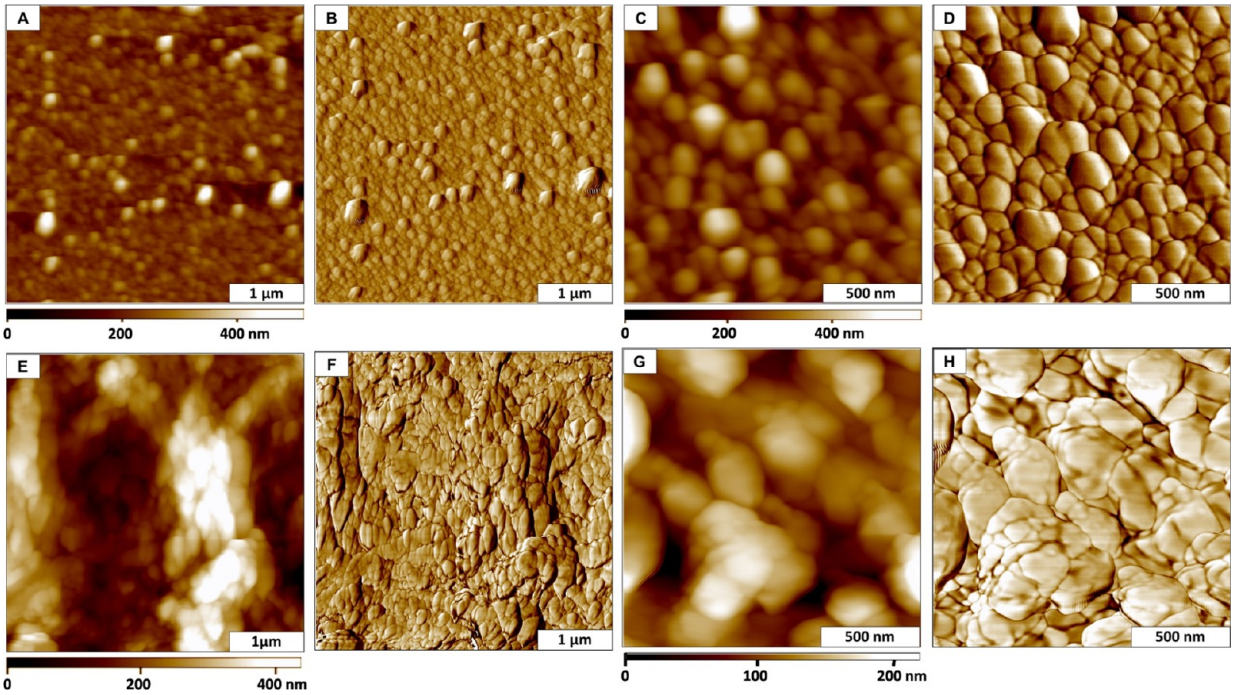

Figure 7. Views of the surface morphology of the electropolymerized films using tapping mode AFM. (A) Topography image of PEDOT (4 × 4 μm^2); (B) simultaneously acquired phase image for A. Zoom-in views (1.5 × 1.5 μm^2) of (C) topography and (D) corresponding phase image of PEDOT thin film. (E) Topograph of thin film **poly(5)** (4 × 4 μm^2); (F) matching phase image; (G) close-up view for thin film **poly(5)** (1.5 × 1.5 μm^2); (H) phase image for G.

polymer in the spectroelectrochemical experiments and agrees with the low impediment for charge carrier formation and transport along better organized semiconducting polymer chains.

An important issue to address at this point is the influence of 2-ethylhexyl solubilizing side chains on the optical and electrochemical properties of **poly(5)**. It is well-documented that thiophene polymers prepared from the monomers incorporating relatively long *n*-alkyl side chains exhibit some properties consistent with the higher ordering along the conjugated backbone and longer conjugation length.[66,72−74] In particular, such polymers commonly show sharper redox peaks in electrochemical data, as well as distinct vibronic structure in absorption spectra in the undoped state. Whereas the complex nature of this phenomenon is not completely understood, it is likely to originate from the interactions between long hydrophobic *n*-alkyl substituents. Such interactions, along with the rigid nature of the polythiophene conjugated backbone, enforce mesogenic behavior of the solid polymer material, therefore increasing ordering and planarization of the conjugated backbone. This phenomenon was recently proven by X-ray diffraction experiments for the case of solution-processed films of poly(didodecylphenylene-dioxythiophene)s,[66] and it is also likely to be valid for the electropolymerized films. Because molecule of **5** possesses two alkyl chains, we could not rule out that a similar "alkyl chain effect" might play role in the distinct electrochemical and spectral properties of **poly(5)**. However, in our design of monomer **5**, we incorporated only the minimal number of side chains—two per monomer—just enough to make it soluble. Thus, unlike all the previous cases where there was at least one long *n*-alkyl group per each thiophene unit (and in some cases there were even two side chains per thiophene unit[66]), the polymer **poly(5)** incorporates only one alkyl chain per four thiophene units. Such a small "fraction" of side chains may not be enough to enforce mesogenic properties in the **poly(5)** films. In such a case, the unusual electrochemical and spectroscopic features of **poly(5)** may be explained by higher molecular order and more narrow distribution of conjugation lengths imposed by the long-chain nature of oligomeric monomer **5**. With the data currently available, we cannot exclude either explanation (or possibility of simultaneous contribution of both effects). The issue is still open at this point; preparing an analogue of **5** with only one solubilizing alkyl chain and comparative studies of the properties of the resulting polymer would be helpful in further discussion, and will be done in the course of future studies.

Atomic Force Microscopy (AFM) and Conductive Probe AFM (CP-AFM) Studies. Scanning probe microscopy was a powerful tool to gain insight into morphology of thin layer of **poly(5)**. A comparison of the surface morphologies of the films of **poly(5)** and PEDOT (prepared by electropolymerization of bisEDOT monomer) potentiodynamically electrodeposited on atomically flat Au surface is presented side-by-side in Figure 7. Simple visual inspection of the tapping mode topography and phase images for the two samples revealed distinct differences in the morphologies of the films. The film of PEDOT showed a uniform distribution of relatively small, tightly packed globular domains with lateral dimensions ranging from 120 to 260 nm (Figure 7A). In contrast, deeper trenches and greater corrugation were characteristic for the film of **poly(5)**, with the discontinuous and less regular, as compared to the PEDOT surface, distribution of irregularly shaped domains (ranging in lateral dimension from 60 to 450 nm). These topographs clearly illustrate the morphological difference between the two films, and likely reflect the difference in molecular organization of these films.

dx.doi.org/10.1021/am301349g | ACS Appl. Mater. Interfaces 2012, 4, 5430−5441

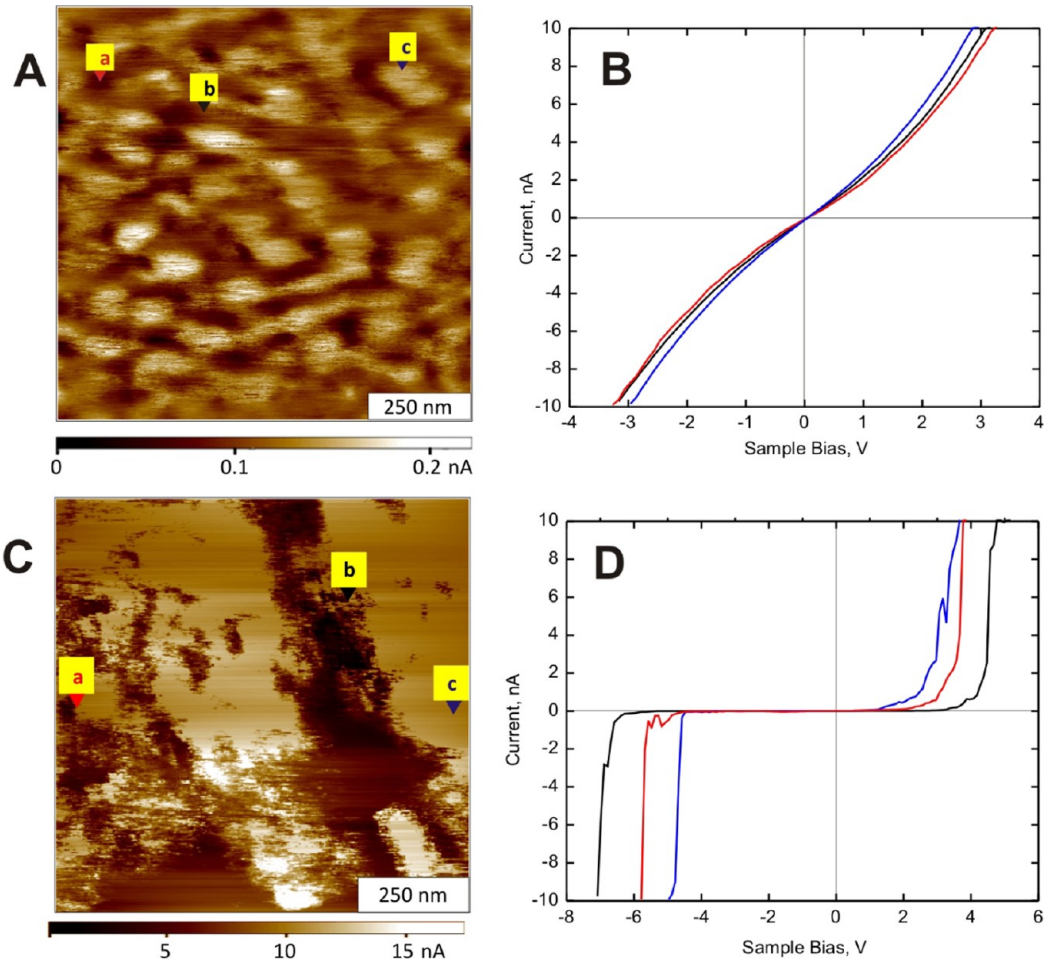

Figure 8. Conductive probe characterizations of PEDOT and **poly(5)** electropolymerized films. (A) Current image of PEDOT (800 × 800 nm^2) acquired with a sample bias of −2 V. Locations are indicated for acquired *I*−*V* spectra (a, red line; b, black line; c, blue line). (B) Overlay of *I*−*V* profiles for the tagged areas in image A; (C) Current image of **poly(5)** (800 × 800 nm^2) acquired with a sample bias of +0.1 V. (D) Plot of *I*−*V* measurements at the marked areas in image C.

Conductive probe (CP-AFM) imaging was previously used to characterize the surface topography and map the conductive domains of the electropolymerized films.[75−78] Current images can be simultaneously acquired with topography by applying a bias voltage to a conductive or semiconductive substrate, and measuring the current with a conductive probe when the tip is placed in contact with the surface of the polymer film.

Characterization using CP-AFM for the electropolymerized film of **poly(5)** and its comparison with electrodeposited PEDOT film are presented in Figure 8. For this study, the polymer films were initially obtained in an electrochemically reduced (undoped) state by keeping the electrodeposited films in supporting electrolyte solution at −1.0 V (vs Ag/Ag$^+$). The details of the surface morphology of the films were not as clearly resolved for the CP-AFM topograph of Figure 8 when compared to the images with tapping mode shown in Figure 7, because the conductive probe is coated with thin layers of titanium and platinum, causing it to be blunt. However, the surface features were still resolvable with the metal-coated tip. Profiles of current−voltage (*I*−*V*) measurements were also acquired at specific sites within the images, and representative *I*−*V* plots for three locations of each film are displayed in Figure 8. These plots revealed remarkable differences between the two polymers. The PEDOT film showed homogeneous and nearly invariant conductivity throughout the entire sample and exhibited noticeably similar symmetry for the positive and negative bias ranges (Figure 8B). This film was conductive throughout the measured voltage levels, demonstrating nearly linear Ohmic conductivity profiles, normally observed for electrodeposited semiconducting polymers.[79−81]

In contrast to the Ohmic conductivity of PEDOT, the thin film of **poly(5)** showed an unusual CP-AFM conductivity pattern. Within the current image, significant changes for the onset of current conduction were observed for the bright versus dark areas of the image (Figure 8C). A representative *I*−*V* plot acquired within the dark area is shown with the black line, whereas example profiles acquired at locations within the brighter areas are colored blue and red (Figure 8D). For the negative bias range, the polymer film remained insulating until highly negative potentials (the onset of conduction occurred between −4 and −7 V depending on the location on the surface), and the transition from nonconducting to conducting form was sharp and exponential. For the positive bias range, the film remained insulating until the threshold potential ranging between 1.8 to 2.5 V was applied (depending on the location of the tip placement) after which the sample would become highly conductive and the *I*−*V* profile changed to a steep, almost vertical line. Such rectification behavior (rectification ratio ∼200 at ±3 V bias for point a in Figure 8C) was typically found for inorganic semiconductor-metal interfaces,[82] but is not

typical for organic semiconducting polymer films. Thus, the film of **poly(5)** behaved as a bias-controlled rectifying switch, sharply changing from insulator to conductor at moderate positive but not negative threshold potentials. This complicated behavior lacks precedents for organic semiconducting polymer films, although similar switching behavior was recently observed in highly organized single-crystalline nanoneedles of conducting polypyrrole, polyaniline, and PEDOT.[83,84] Although the detailed understanding of this phenomenon requires further experimental and theoretical studies, the sharp insulator−conductor transition may indeed reflect an increased molecular organization, and/or higher ordered bulk morphology of the thin-film **poly(5)**. Indeed, whereas typical molecular rectifiers (Aviram-Ratner diodes) possess the interconnected donor−acceptor (D-A) pairs,[85] it has been recently shown that this is not the only possibility, and organic compounds without an intramolecular D−A junction can also show asymmetric conduction patterns.[86] One (more common) case involves formation of Schottky barriers at metal electrode − organic interfaces (similar to inorganic semiconductor−metal interfaces); this possibility should, however, be ruled out for **poly(5)** because the chemically similar PEDOT polymer was found to form purely Ohmic contacts at exactly the same experimental conditions. Another, more rarely observed situation of rectifying behavior arises when the organic molecules are placed asymmetrically in the metal−molecule−metal junction.[87,88] For the case of a bulk conducting film, this means a uniform orientation of the polymer molecules, at least in the area of the AFM tip contact. Thus, the experimentally found rectifying bias-switch behavior of **poly(5)**'s thin films as compared to the Ohmic behavior of the films of PEDOT may reflect more ordered organization in the former. The observed location-dependent variations in the turn-on switching bias are possibly due to differences in the extent of molecular order, as well as π-electron conjugation, degree of polymerization, etc., between various domains of the **poly(5)** thin film. With limited experimental data available, no rigorous conclusion regarding the reasons for this unusual electrical behavior can be drawn at this time, and more experiments will have to be done to gain better understanding of this phenomenon.

CONCLUSIONS

A series of soluble EDOT-based H-terminated oligomers ranging in length from four to eight EDOT/thiophene units was prepared and analyzed by experimental and computational techniques. Both experimentally observed and computed properties of the oligomers were consistent with highly conjugated predominantly planar solution conformation (mostly due to hyperconjugative intramolecular interactions as revealed by computational NBO analysis) allowing for high stabilization of cation radical intermediates. Despite the increasing stabilization of the reactive cation radical species in extended π-electron conjugated oligomers, the longest oligomer **5** was found to be easily electropolymerizable yielding stable semiconducting polymer film. This electrodeposited film showed some interesting and unusual optical and electrical properties consistent with the possibility of improved molecular order along the conjugated backbone, decreased number of defects in its π-electron conjugated system along with longer and more uniform effective conjugation length, and more narrow distribution of chain lengths (lower polydispersity). The efficient electropolymerization of **5** was in good agreement with our initial hypothesis that a reactive trication radical species can be readily formed in sufficiently long oligomers, therefore making them electropolymerizable. Thus, extending oligothiophene length beyond certain limit apparently brings them to an "island of reactivity" toward electropolymerization. While synthetic preparation of long-chain oligomers for fabrication of polymer thin films by electropolymerization is a cost- and labor-intensive process, the possibility to use these oligomers to make semiconducting polymer materials with advanced electronic properties may in some instances outweigh the cost of their synthesis. Further studies on the generality of the trication radical induced electropolymerization of long-chain conjugated oligothiophenes, as well as comparison of properties of resulting polymer films, require preparation and studies of even longer EDOT-containing and purely thiophene oligomers, which is currently underway in our laboratory.

ASSOCIATED CONTENT

Supporting Information

Detailed synthetic and experimental procedures, additional figures, and crystallographic data for compound **1** (CIF). This material is available free of charge via the Internet at http://pubs.acs.org.

AUTHOR INFORMATION

Corresponding Author

*E-mail: een@lsu.edu.

Present Address

[†]Sri Lanka Institute of Nanotechnology, Lot 14, Zone 1, Biyagama Export Processing Zone, Malwana, Sri Lanka.

Notes

The authors declare no competing financial interest.

ACKNOWLEDGMENTS

This work was supported by the National Science Foundation (Grant DMR-1006336).

REFERENCES

(1) Otsubo, T.; Aso, Y.; Takimiya, K. *J. Mater. Chem.* **2002**, *12*, 2565−2575.
(2) Surin, M.; Leclère, P.; De Feyter, S.; Abdel-Mottaleb, M. M. S.; De Schryver, F. C.; Henze, O.; Feast, W. J.; Lazzaroni, R. *J. Phys. Chem. B* **2006**, *110*, 7898−7908.
(3) Yasuda, T.; Ooi, H.; Morita, J.; Akama, Y.; Minora, K.; Funahashi, M.; Shimomura, T.; Kato, T. *Adv. Funct. Mater.* **2009**, *19*, 411−419.
(4) Katz, H. E.; Bao, Z.; Gilat, S. L. *Acc. Chem. Res.* **2001**, *34*, 359−369.
(5) Facchetti, A.; Yoon, M.-H.; Stern, C. L.; Hutchison, G. R.; Ratner, M. A.; Marks, T. J. *J. Am. Chem. Soc.* **2004**, *126*, 13480−13501.
(6) Zotti, G.; Vercelli, B.; Berlin, A. *Acc. Chem. Res.* **2008**, *41*, 1098−1109.
(7) Jones, B. A.; Facchetti, A.; Wasielewski, M. R.; Marks, T. J. *J. Am. Chem. Soc.* **2007**, *129*, 15259−15278.
(8) Perepichka, I. F.; Perepichka, D. F.; Meng, H.; Wudl, F. *Adv. Mater.* **2005**, *17*, 2281−2305.
(9) Murphy, A. R.; Fréchet, J. M. J. *Chem. Rev.* **2007**, *107*, 1066−1096.
(10) Lin, Y.; Li, Y.; Zhan, X. *Chem. Soc. Rev.* **2012**, *41*, 4245−4272.
(11) Facchetti, A. *Mater. Today* **2007**, *10*, 28−37.
(12) Tan, S.; Zhai, J.; Fang, H.; Jiu, T.; Ge, J.; Li, Y.; Jiang, L.; Zhu, D. *Chem.—Eur. J.* **2005**, *11*, 6272−6276.
(13) Noma, N.; Tsuzuki, T.; Shirota, Y. *Adv. Mater.* **1995**, *7*, 647−648.

(14) Cicoira, F.; Santato, C.; Melucci, M.; Favaretto, L.; Gazzano, M.; Muccini, M.; Barbarella, G. *Adv. Mater.* **2006**, *18*, 169−174.
(15) Briehn, C. A.; Schiedel, M.-C.; Bonsen, E. M.; Schuhmann, W.; Bäuerle, P. *Angew. Chem., Int. Ed.* **2001**, *40*, 4680−4683.
(16) Kim, D. H.; Lee, B.-L.; Moon, H.; Kang, H. M.; Jeong, E. J.; Park, J.-I.; Han, K.-M.; Lee, S.; Yoo, B. W.; Koo, B. W.; Kim, J. Y.; Lee, W. H.; Cho, K.; Becerril, H. A.; Bao, Z. *J. Am. Chem. Soc.* **2009**, *131*, 6124−6132.
(17) Beryozkina, T.; Senkovskyy, V.; Kaul, E.; Kiriy, A. *Macromolecules* **2008**, *41*, 7817−7823.
(18) Usta, H.; Risko, C.; Wang, Z.; Huang, H.; Deliomeroglu, M. K.; Zhukhovitskiy, A.; Facchetti, A.; Marks, T. J. *J. Am. Chem. Soc.* **2009**, *131*, 5586−5608.
(19) Binauld, S.; Damiron, D.; Connal, L. A.; Hawker, C. J.; Drockenmuller, E. *Macromol. Rapid Commun.* **2011**, *32*, 147−168.
(20) Tour, J. M. *Chem. Rev.* **1996**, *96*, 537−553.
(21) Martin, R. E.; Diederich, F. *Angew. Chem., Int. Ed.* **1999**, *38*, 1350−1377.
(22) Mishra, A.; Ma, C.-Q.; Bäuerle, P. *Chem. Rev.* **2009**, *109*, 1141−1276.
(23) Audebert, P.; Miomandre, F. Electrochemistry of conducting polymers. In: *Handbook of Conducting Polymers*, 3rd ed.; Skotheim, T. A., Reynolds, J. R., Eds.; CRC Press: Boca Raton, FL, 2007; Vol. *1*, 18−1−18−40.
(24) Gurunathan, K.; Murugan, A. V.; Marimuthu, R.; Mulik, U. P.; Amalnerkar, D. P. *Mater. Chem. Phys.* **1999**, *61*, 173−191.
(25) Roncali, J. *J. Mater. Chem.* **1999**, *9*, 1875−1893.
(26) Manceau, M.; Rivaton, A.; Gardette, J. L.; Guillerez, S.; Lemaître, N. *Polym. Degrad. Stab.* **2009**, *94*, 898−907.
(27) Chambon, S.; Rivaton, A.; Gardette, J. L.; Firon, M.; Lutsen, L. *J. Polym. Sci., Part A: Polym. Chem.* **2007**, *45*, 317−331.
(28) Zotti, G.; Schiavon, G. *Chem. Mater.* **1993**, *5*, 430−436.
(29) Zotti, G.; Gallazzi, M. C.; Zerbi, G.; Meille, S. V. *Synth. Met.* **1995**, *73*, 217−225.
(30) Caspar, J. V.; Ramamurthy, V.; Corbin, D. R. *J. Am. Chem. Soc.* **1991**, *113*, 600−610.
(31) Audebert, P.; Catel, J.-M.; Le Coustumer, G.; Duchenet, V.; Hapiot, P. *J. Phys. Chem.* **1995**, *99*, 11923−11929.
(32) Audebert, P.; Catel, J.-M.; Le Coustumer, G.; Duchenet, V.; Hapiot, P. *J. Phys. Chem. B* **1998**, *102*, 8661−8669.
(33) Audebert, P.; Catel, J.-M.; Duchenet, V.; Guyard, L.; Hapiot, P.; Le Coustumer, G. *Synth. Met.* **1999**, *101*, 642−645.
(34) Brillas, E.; Oliver, R.; Estrany, F.; Rodríguez, E.; Tejero, S. *Electrochim. Acta* **2002**, *47*, 1623−1631.
(35) Delabouglise, D.; Hmyene, M.; Horowitz, G.; Yassar, A.; Garnier, F. *Adv. Mater.* **1992**, *4*, 107−110.
(36) Meerholz, K.; Heinze, J. *Electrochim. Acta* **1996**, *41*, 1839−1854.
(37) Sotzing, G. A.; Reynolds, J. R. *Chem. Mater.* **1996**, *8*, 882−889.
(38) Perepichka, I. F.; Roquet, S.; Leriche, P.; Raimundo, J.-M.; Frère, P.; Roncali, J. *Chem.—Eur. J.* **2006**, *12*, 2960−2966.
(39) Rohde, D.; Dunsch, L.; Tabet, A.; Hartmann, H.; Fabian, J. *J. Phys. Chem. B* **2006**, *110*, 8223−8231.
(40) Casado, J.; Delgado, M. C. R.; Shirota, Y.; Hernández, V.; Navarrete, J. T. L. *J. Phys. Chem. B* **2003**, *107*, 2637−2644.
(41) Casado, J.; Miller, L. L.; Mann, K. R.; Pappenfus, T. M.; Hernández, V.; Navarrete, J. T. L. *J. Phys. Chem. B* **2002**, *106*, 3597−3605.
(42) Hapiot, P.; Lagrost, C.; Le Floch, F.; Raoult, E.; Rault-Berthelot, J. *Chem. Mater.* **2005**, *17*, 2003−2012.
(43) Domagala, W.; Lapkowski, M.; Guillerez, S.; Bidan, G. *Electrochim. Acta* **2003**, *48*, 2379−2388.
(44) Leclerc, M.; Diaz, F. M.; Wegner, G. *Makromol. Chem.* **1989**, *190*, 3105−3116.
(45) Larmat, F.; Reynolds, J. R.; Reinhardt, B. A.; Brott, L. L.; Clarson, S. J. *J. Polym. Sci., Part A: Polym. Chem.* **1997**, *35*, 3627−3636.
(46) Piron, F.; Leriche, P.; Grosu, I.; Roncali, J. *J. Mater. Chem.* **2010**, *20*, 10260−10268.
(47) Taerum, T.; Lukoyanova, O.; Wylie, R. G.; Perepichka, D. F. *Org. Lett.* **2009**, *11*, 3230−3233.
(48) Turbiez, M.; Frère, P.; Allain, M.; Videlot, C.; Ackermann, J.; Roncali, J. *Chem.—Eur. J.* **2005**, *11*, 3742−3752.
(49) Apperloo, J. J.; Groenendaal, L. B.; Verheyen, H.; Jayakannan, M.; Janssen, R. A. J.; Dkhissi, A.; Beljonne, D.; Lazzaroni, R.; Brédas, J.-L. *Chem.—Eur. J.* **2002**, *8*, 2384−2396.
(50) Turbiez, M.; Hergué, N.; Leriche, P.; Frère, P. *Tetrahedron Lett.* **2009**, *50*, 7148−7151.
(51) Lin, C.; Endo, T.; Takase, M.; Iyoda, M.; Nishinaga, T. *J. Am. Chem. Soc.* **2011**, *133*, 11339−11350.
(52) Olmsted, J., III *J. Phys. Chem.* **1979**, *83*, 2581−2584.
(53) Frisch, M. J.; Trucks, G. W.; Schlegel, H. B.; Scuseria, G. E.; Robb, M. A.; Cheeseman, J. R.; Montgomery, Jr., J. A.; Vreven, T.; Kudin, K. N.; Burant, J. C.; Millam, J. M.; Iyengar, S. S.; Tomasi, J.; Barone, V.; Mennucci, B.; Cossi, M.; Scalmani, G.; Rega, N.; Petersson, G. A.; Nakatsuji, H.; Hada, M.; Ehara, M.; Toyota, K.; Fukuda, R.; Hasegawa, J.; Ishida, M.; Nakajima, T.; Honda, Y.; Kitao, O.; Nakai, H.; Klene, M.; Li, X.; Knox, J. E.; Hratchian, H. P.; Cross, J. B.; Bakken, V.; Adamo, C.; Jaramillo, J.; Gomperts, R.; Stratmann, R. E.; Yazyev, O.; Austin, A. J.; Cammi, R.; Pomelli, C.; Ochterski, J. W.; Ayala, P. Y.; Morokuma, K.; Voth, G. A.; Salvador, P.; Dannenberg, J. J.; Zakrzewski, V. G.; Dapprich, S.; Daniels, A. D.; Strain, M. C.; Farkas, O.; Malick, D. K.; Rabuck, A. D.; Raghavachari, K.; Foresman, J. B.; Ortiz, J. V.; Cui, Q.; Baboul, A. G.; Clifford, S.; Cioslowski, J.; Stefanov, B. B.; Liu, G.; Liashenko, A.; Piskorz, P.; Komaromi, I.; Martin, R. L.; Fox, D. J.; Keith, T.; Al-Laham, M. A.; Peng, C. Y.; Nanayakkara, A.; Challacombe, M.; Gill, P. M. W.; Johnson, B.; Chen, W.; Wong, M. W.; Gonzalez, C.; Pople, J. A. *Gaussian 03, Revision D.02*; Gaussian, Inc.: Wallingford CT, 2004.
(54) Wilcox, D.; Dove, B.; McDavid, D.; Greer, D. *UTHSCSA Image Tool for Windows version 3.00*; The University of Texas Health Science Center: San Antonio, TX, 1995−2002.
(55) Zade, S. S.; Zamoshchik, N.; Bendikov, M. *Acc. Chem. Res.* **2011**, *44*, 14−24.
(56) Roncali, J.; Blanchard, P.; Frère, P. *J. Mater. Chem.* **2005**, *15*, 1589−1610.
(57) Medina, B. M.; Wasserberg, D.; Meskers, S. C. J.; Mena-Osteritz, E.; Bäuerle, P.; Gierschner, J. *J. Phys. Chem. A* **2008**, *112*, 13282−13286.
(58) Weinhold, F. Natural bond orbital methods. In: *Encyclopedia of Computational Chemistry*; Schleyer, P. v. R., Allinger, N. L., Clark, T., Gasteiger, J., Kollman, P. A., Schaefer III, H. F., Schreiner, P. R., Eds.; Wiley: Chichester: U.K., 1998; Vol. *3*, pp 1792−1811.
(59) Alemán, C.; Armelin, E.; Iribarren, J. I.; Liesa, F.; Laso, M.; Casanovas, J. *Synth. Met.* **2005**, *149*, 151−156.
(60) Wasserberg, D.; Meskers, S. C. J.; Janssen, R. A. J.; Mena-Osteritz, E.; Bäuerle, P. *J. Am. Chem. Soc.* **2006**, *128*, 17007−17017.
(61) Akoudad, S.; Roncali, J. *Synth. Met.* **1998**, *93*, 111−114.
(62) Groenendaal, L. B.; Jonas, F.; Freitag, D.; Pielartzik, H.; Reynolds, J. R. *Adv. Mater.* **2000**, *12*, 481−494.
(63) Zade, S. S.; Bendikov, M. *Org. Lett.* **2006**, *8*, 5243−5246.
(64) Groenendaal, L. B.; Zotti, G.; Aubert, P.-H.; Waybright, S. M.; Reynolds, J. R. *Adv. Mater.* **2003**, *15*, 855−879.
(65) Kim, Y.; Cook, S.; Tuladhar, S. M.; Choulis, S. A.; Nelson, J.; Durrant, J. R.; Bradley, D. D. C.; Giles, M.; McCulloch, I.; Ha, C.-S.; Ree, M. *Nat. Mater.* **2006**, *5*, 197−203.
(66) Grenier, C. R. G.; Pisula, W.; Joncheray, T. J.; Müllen, K.; Reynolds, J. R. *Angew. Chem., Int. Ed.* **2007**, *46*, 714−717.
(67) Kim, S.-S.; Na, S.-I.; Jo, J.; Tae, G.; Kim, D.-Y. *Adv. Mater.* **2007**, *19*, 4410−4415.
(68) Nesterov, E. E.; Zhu, Z.; Swager, T. M. *J. Am. Chem. Soc.* **2005**, *127*, 10083−10088.
(69) Zhu, Z.; Swager, T. M. *J. Am. Chem. Soc.* **2002**, *124*, 9670−9671.
(70) Kittlesen, G. P.; White, H. S.; Wrighton, M. S. *J. Am. Chem. Soc.* **1984**, *106*, 7389−7396.
(71) Simone, D. L.; Swager, T. M. *J. Am. Chem. Soc.* **2000**, *122*, 9300−9301.
(72) Groenendaal, L.; Zotti, G.; Jonas, F. *Synth. Met.* **2001**, *118*, 105−109.

(73) Havinga, E. E.; Mutsaers, C. M. J.; Jenneskens, L. W. *Chem. Mater.* **1996**, *8*, 769−776.
(74) Sankaran, B.; Reynolds, J. R. *Macromolecules* **1997**, *30*, 2582−2588.
(75) Klein, D. L.; McEuen, P. L.; Bowen-Katari, J. E.; Alivisatos, A. P. *Nanotechnology* **1996**, *7*, 397−400.
(76) Klein, D. L.; McEuen, P. L. *Appl. Phys. Lett.* **1995**, *66*, 2478−2480.
(77) Wold, D. J.; Frisbie, C. D. *J. Am. Chem. Soc.* **2000**, *122*, 2970−2971.
(78) Rawlett, A. M.; Hopson, T. J.; Nagahar, L. A.; Tsui, R. K.; Ramachandran, G. K.; Lindsay, S. M. *Appl. Phys. Lett.* **2002**, *81*, 3043−3045.
(79) Barrière, F.; Fabre, B.; Hao, E.; LeJeune, Z. M.; Hwang, E.; Garno, J. C.; Nesterov, E. E.; Vicente, M. G. H. *Macromolecules* **2009**, *42*, 2981−2987.
(80) Lee, H. J.; Park, S.-M. *J. Phys. Chem. B* **2004**, *108*, 1590−1595.
(81) Wu, C.-G.; Chang, S.-S. *J. Phys. Chem. B* **2005**, *109*, 825−832.
(82) Park, W. I.; Yi, G.-C.; Kim, J.-W.; Park, S.-M. *Appl. Phys. Lett.* **2003**, *82*, 4358−4360.
(83) Su, K.; Nuraje, N.; Zhang, L.; Chu, I.-W.; Peetz, R. M.; Matsui, H.; Yang, N.-L. *Adv. Mater.* **2007**, *19*, 669−672.
(84) Nuraje, N.; Su, K.; Yang, N.-I.; Matsui, H. *ACS Nano* **2008**, *2*, 502−506.
(85) Aviram, A.; Ratner, M. A. *Chem. Phys. Lett.* **1974**, *29*, 277−283.
(86) Chabinyc, M. L.; Chen, X.; Holmlin, R. E.; Jacobs, H.; Skulason, H.; Frisbie, C. D.; Mujica, V.; Ratner, M. A.; Rampi, M. A.; Whitesides, G. M. *J. Am. Chem. Soc.* **2002**, *124*, 11730−11736.
(87) Metzger, R. M. *Chem. Rev.* **2003**, *103*, 3803−3834.
(88) Vercelli, B.; Zotti, G.; Berlin, A.; Grimoldi, S. *Chem. Mater.* **2006**, *18*, 3754−3763.